

## supporting information

### **Reprogramming the redox states of nickel via interface engineering and heteroatom doping to boost overall water splitting**

Wei Lai<sup>†</sup>, Lihong Ge<sup>†</sup>, Hua Yang<sup>†</sup>, Yilin Deng<sup>†,\*</sup>, Huaming Li<sup>†</sup>, Bo Ouyang<sup>||</sup>, Li Xu<sup>†</sup>, Jian Bao<sup>†</sup>

<sup>†</sup>Institute for Energy Research, Jiangsu University, Zhenjiang 212013, China

<sup>||</sup>Department of Applied Physics and Institution of Energy and Microstructure, Nanjing University of  
Science and Technology, Nanjing 210094, China

\* Correspondence should be addressed to: yldeng@ujs.edu.cn (YD)

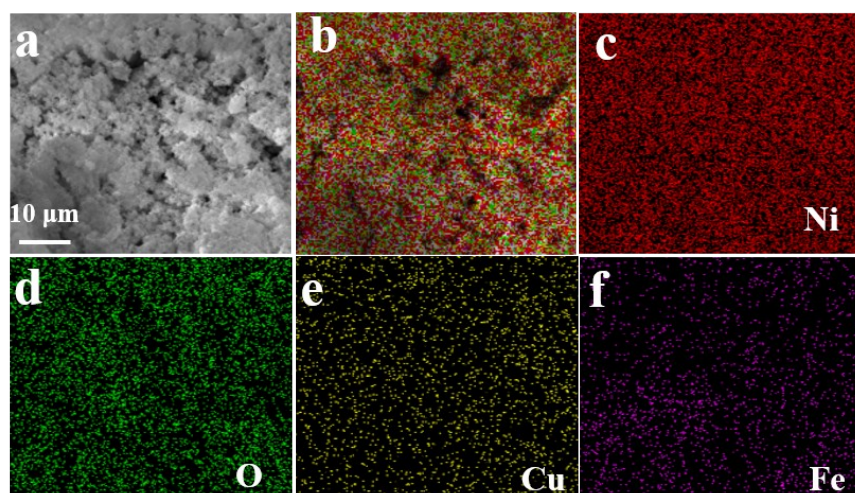


**Figure S1.** (a) The SEM and (b-f) corresponding elemental mapping of EO-Cu<sub>3</sub>-Fe<sub>2</sub>-Ni<sub>50</sub>/NF.

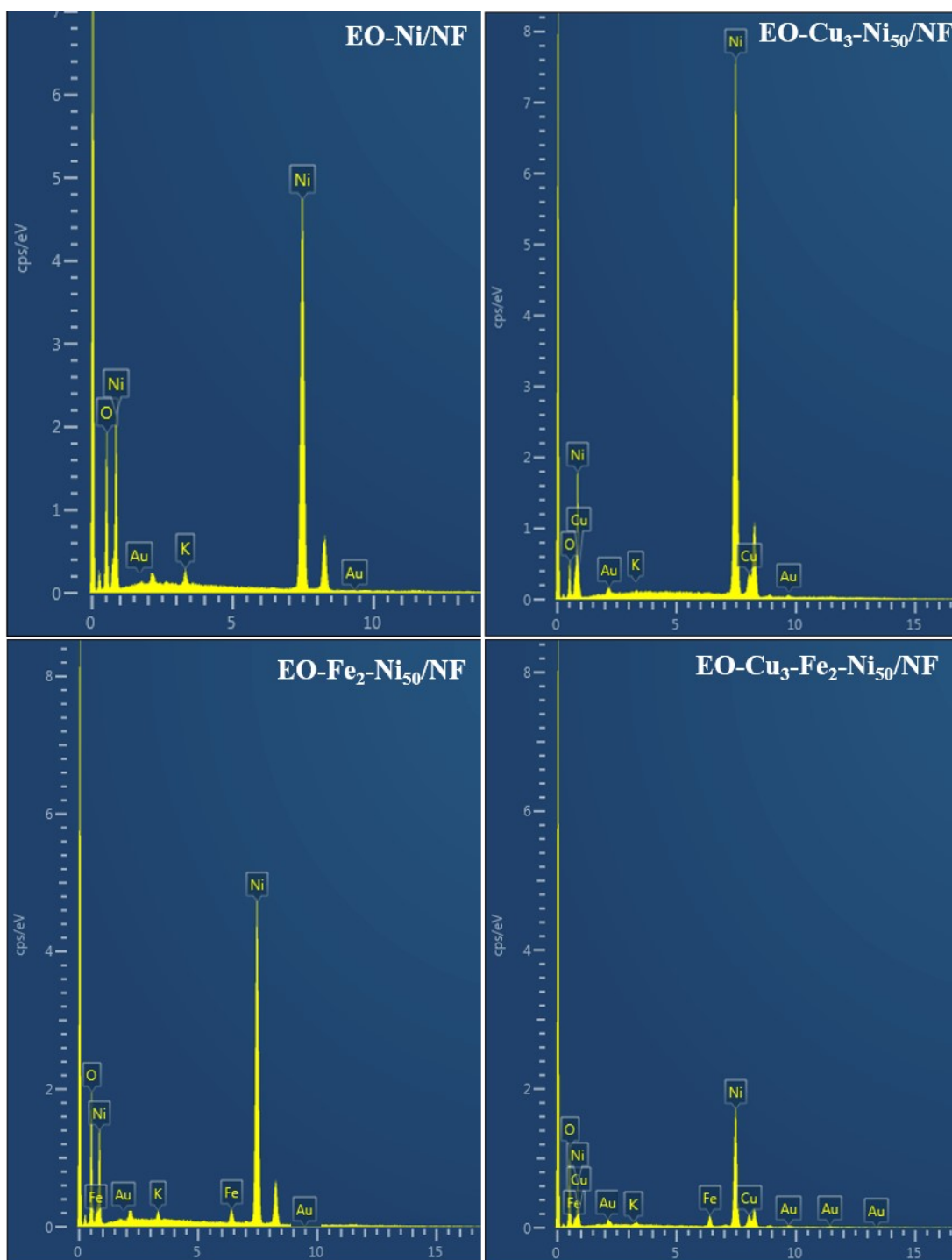


**Figure S2.** EDS of EO-Ni/NF, EO-Cu<sub>3</sub>-Ni<sub>50</sub>/NF, EO-Fe<sub>2</sub>-Ni<sub>50</sub>/NF and EO-Cu<sub>3</sub>-Fe<sub>2</sub>-Ni<sub>50</sub>/NF. (Potassium element came from the KOH electrolyte for electrochemical oxidation treatment. Besides, in order to better characterize the surface morphology of the samples, gold was sprayed on the surfaces of the samples to increase their conductivity, hence leading to the appearance of gold element in the spectra.)

**Table S1.** Atomic ratios of different metals in EO-Ni/NF, EO-Cu<sub>3</sub>-Ni<sub>50</sub>/NF, EO-Fe<sub>2</sub>-Ni<sub>50</sub>/NF and EO-Cu<sub>3</sub>-Fe<sub>2</sub>-Ni<sub>50</sub>/NF recorded by ICP-OES.

Catalysts	at (%)			Cu: Fe: Ni
	Cu	Fe	Ni	
EO-Ni/NF	0	0	100	-----
EO-Cu <sub>3</sub> -Ni <sub>50</sub> /NF	4.65	0	95.35	Cu: Ni =1.0 : 20.5
EO-Fe <sub>2</sub> -Ni <sub>50</sub> /NF	0	1.59	98.41	Fe: Ni =1.0 : 61.9
EO-Cu <sub>3</sub> -Fe <sub>2</sub> -Ni <sub>50</sub> /NF	7.81	2.98	89.21	Cu: Fe: Ni=2.6: 1.0: 29.9

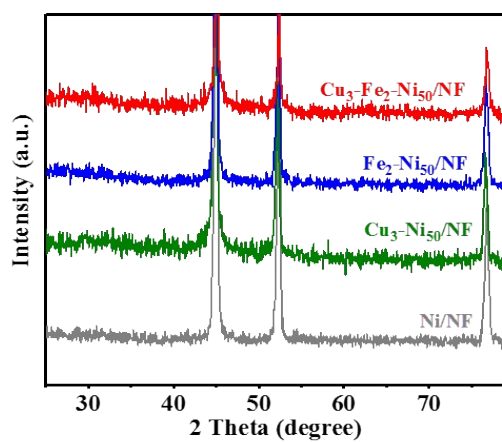


**Figure S3.** The XRD patterns of Ni/NF, Cu<sub>3</sub>-Ni<sub>50</sub>/NF, Fe<sub>2</sub>-Ni<sub>50</sub>/NF and Cu<sub>3</sub>-Fe<sub>2</sub>-Ni<sub>50</sub>/NF.

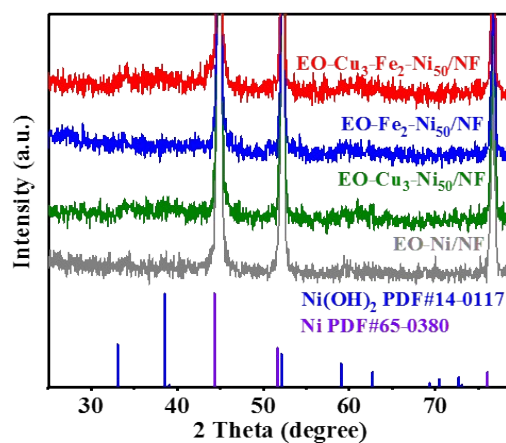


**Figure S4.** The XRD patterns of EO-Ni/NF, EO-Cu<sub>3</sub>-Ni<sub>50</sub>/NF, EO-Fe<sub>2</sub>-Ni<sub>50</sub>/NF and EO-Cu<sub>3</sub>-Fe<sub>2</sub>-Ni<sub>50</sub>/NF.

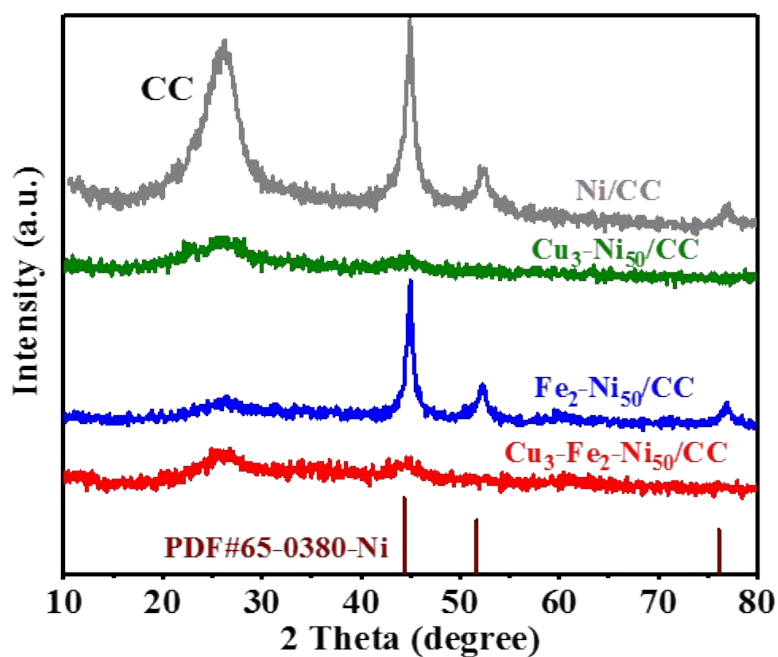


**Figure S5.** The XRD patterns of Ni/CC, Cu<sub>3</sub>-Ni<sub>50</sub>/CC, Fe<sub>2</sub>-Ni<sub>50</sub>/CC and Cu<sub>3</sub>-Fe<sub>2</sub>-Ni<sub>50</sub>/CC (CC represents for carbon cloth).

Note that Ni/CC and Fe<sub>2</sub>-Ni<sub>50</sub>/CC show obvious diffraction peaks at 44.5°, 51.8° and 76.4°, while Cu<sub>3</sub>-Ni<sub>50</sub>/CC and Cu<sub>3</sub>-Fe<sub>2</sub>-Ni<sub>50</sub>/CC only appear one peak at 44.5°, with a broader shape as compare to that on the Ni/CC and Fe<sub>2</sub>-Ni<sub>50</sub>/CC. This may be because that particle refinement due to the addition of Cu reduces the crystallinity of the catalyst and affects the diffraction.<sup>1</sup>

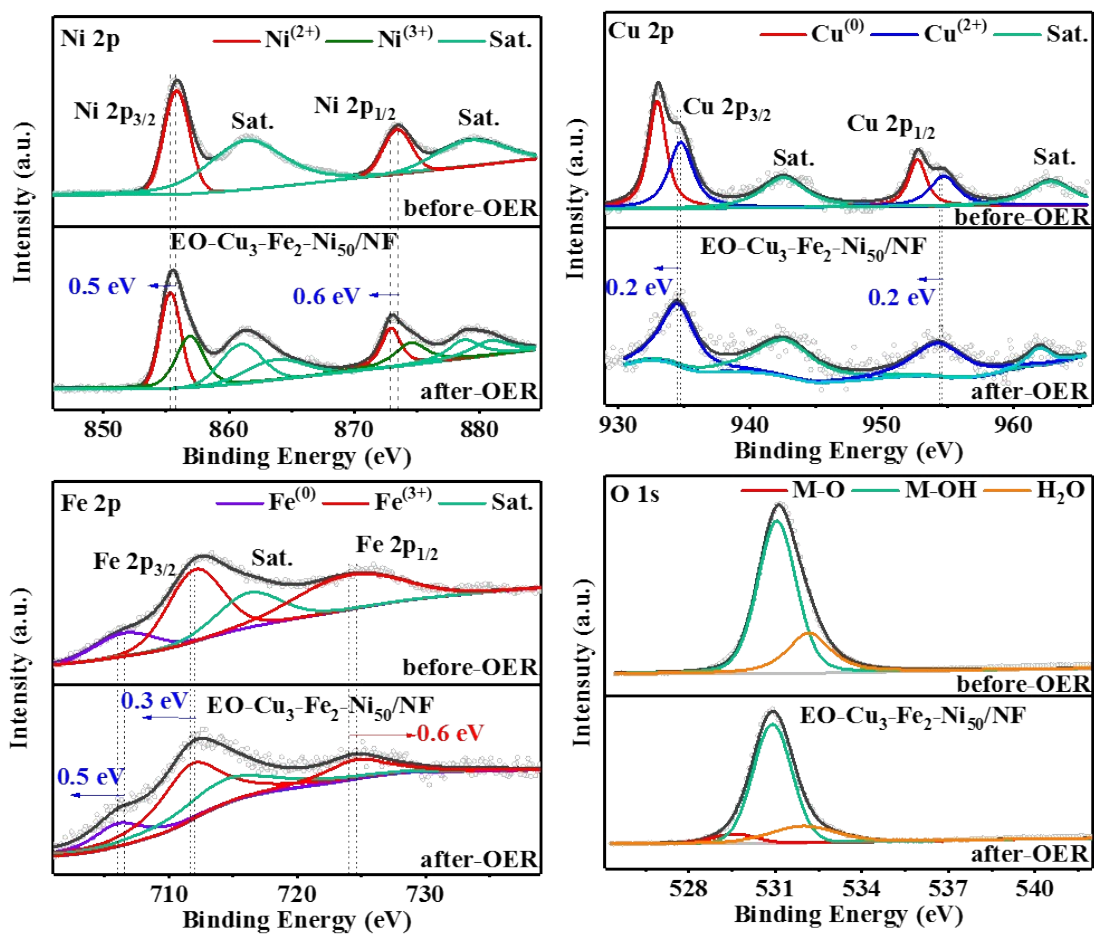


**Figure S6.** (a) Ni 2p, (b) Cu 2p, (c) Fe 2p and (d) O 1s XPS spectra of EO-Cu<sub>3</sub>-Fe<sub>2</sub>-Ni<sub>50</sub>/NF after OER measurement.

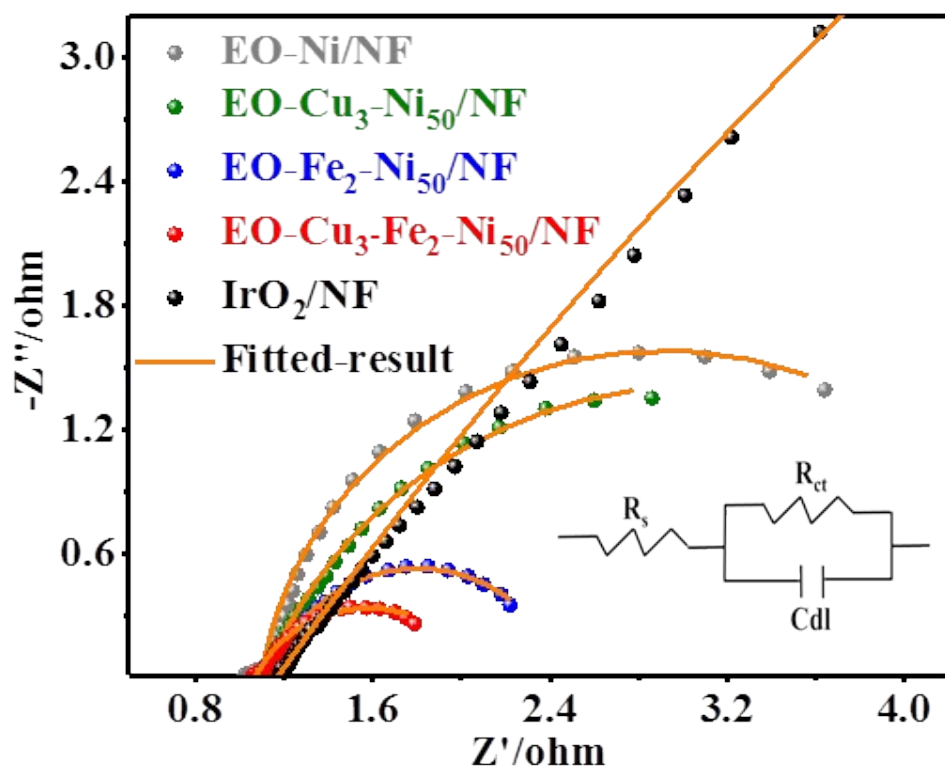


**Figure S7.** The equivalent circuit and the detail simulated results in EIS for OER.



**Table S2.** Charge transfer resistance ( $R_{ct}$ ) and solution resistance ( $R_s$ ) obtained from the equivalent circuit models of different samples.

<b>Catalysts (OER)</b>	<b><math>R_s / \Omega</math></b>	<b><math>R_{ct} / \Omega</math></b>
EO-Ni/NF	1.1	4.0
EO-Cu <sub>3</sub> -Ni <sub>50</sub> /NF	1.1	3.6
EO-Fe <sub>2</sub> -Ni <sub>50</sub> /NF	1.1	1.3
EO-Cu <sub>3</sub> -Fe <sub>2</sub> -Ni <sub>50</sub> /NF	1.1	1.0
IrO <sub>2</sub> /NF	1.1	40.0
<b>Catalysts (HER)</b>	<b><math>R_s / \Omega</math></b>	<b><math>R_{ct} / \Omega</math></b>
EO-Ni/NF	1.1	2.1
EO-Cu <sub>3</sub> -Ni <sub>50</sub> /NF	1.1	1.2
EO-Fe <sub>2</sub> -Ni <sub>50</sub> /NF	1.1	2.0
EO-Cu <sub>3</sub> -Fe <sub>2</sub> -Ni <sub>50</sub> /NF	1.1	0.9
Pt/C/NF	1.1	0.6

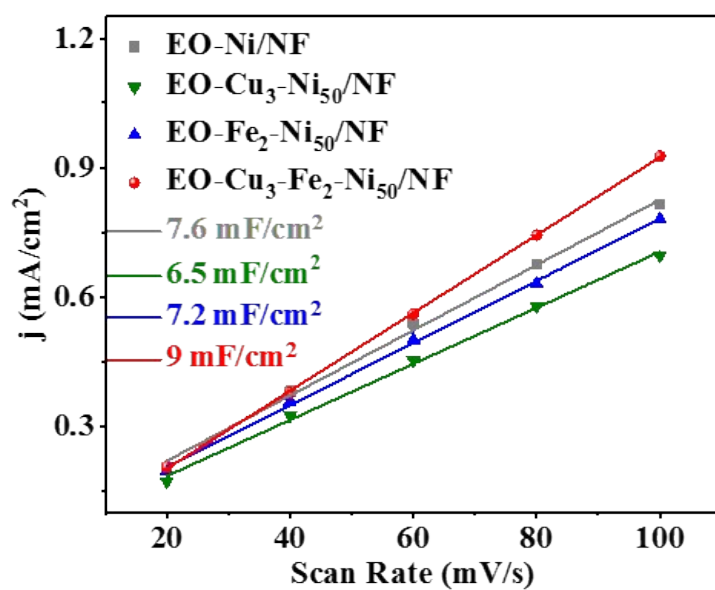


**Figure S8.** The electrochemical double-layer capacitances ( $C_{dl}$ ) of EO-Ni/NF, EO-Cu<sub>3</sub>-Ni<sub>50</sub>/NF, EO-Fe<sub>2</sub>-Ni<sub>50</sub>/NF and EO-Cu<sub>3</sub>-Fe<sub>2</sub>-Ni<sub>50</sub>/NF for OER.

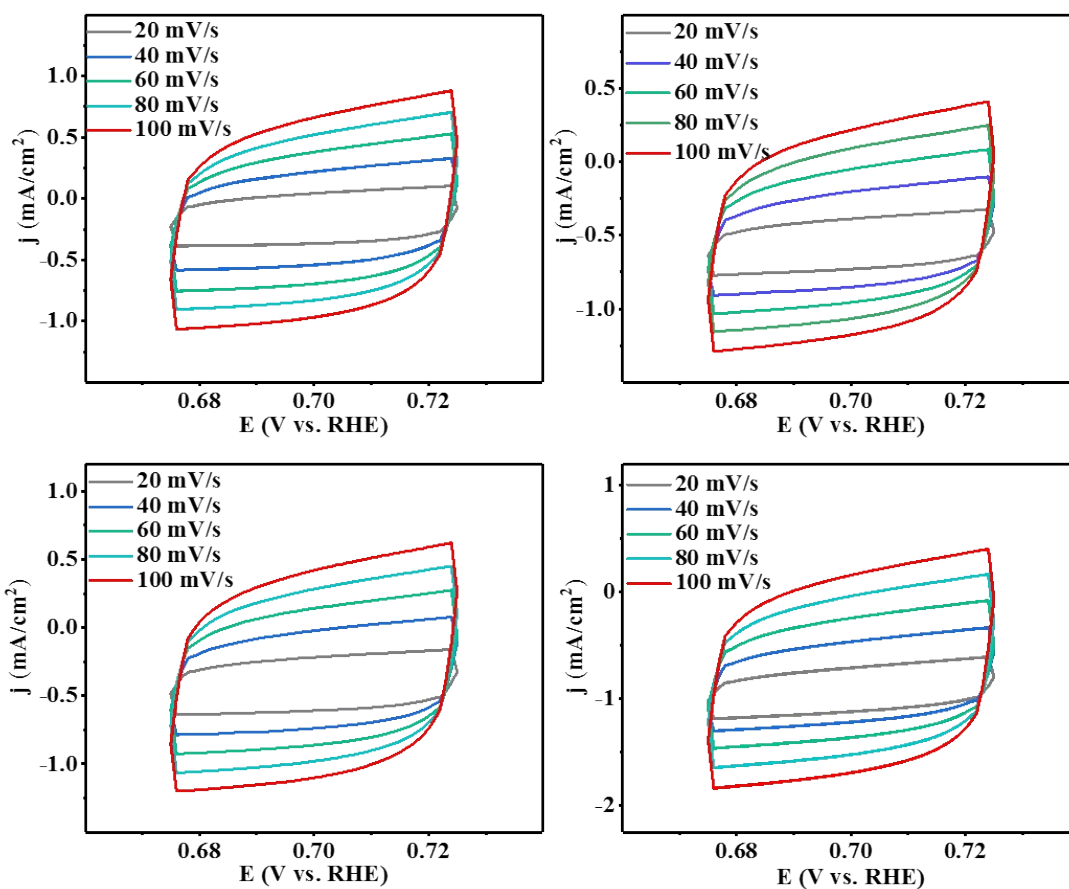


**Figure S9.** The CVs of (a) EO-Ni/NF, (b) EO-Cu<sub>3</sub>-Ni<sub>50</sub>/NF, (c) EO-Fe<sub>2</sub>-Ni<sub>50</sub>/NF and (d) EO-Cu<sub>3</sub>-Fe<sub>2</sub>-Ni<sub>50</sub>/NF at different scan rates in the non-Faraday region (0.675 ~0.725 V).

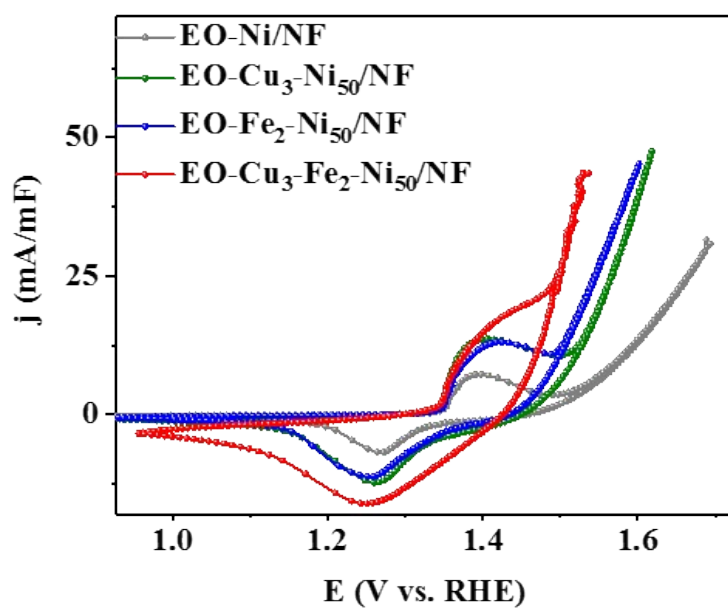


**Figure S10.** The normalized CV curves of EO-Ni/NF, EO-Cu<sub>3</sub>-Ni<sub>50</sub>/NF, EO-Fe<sub>2</sub>-Ni<sub>50</sub>/NF and EO-Cu<sub>3</sub>-Fe<sub>2</sub>-Ni<sub>50</sub>/NF for OER by their respective  $C_{dl}$  values.

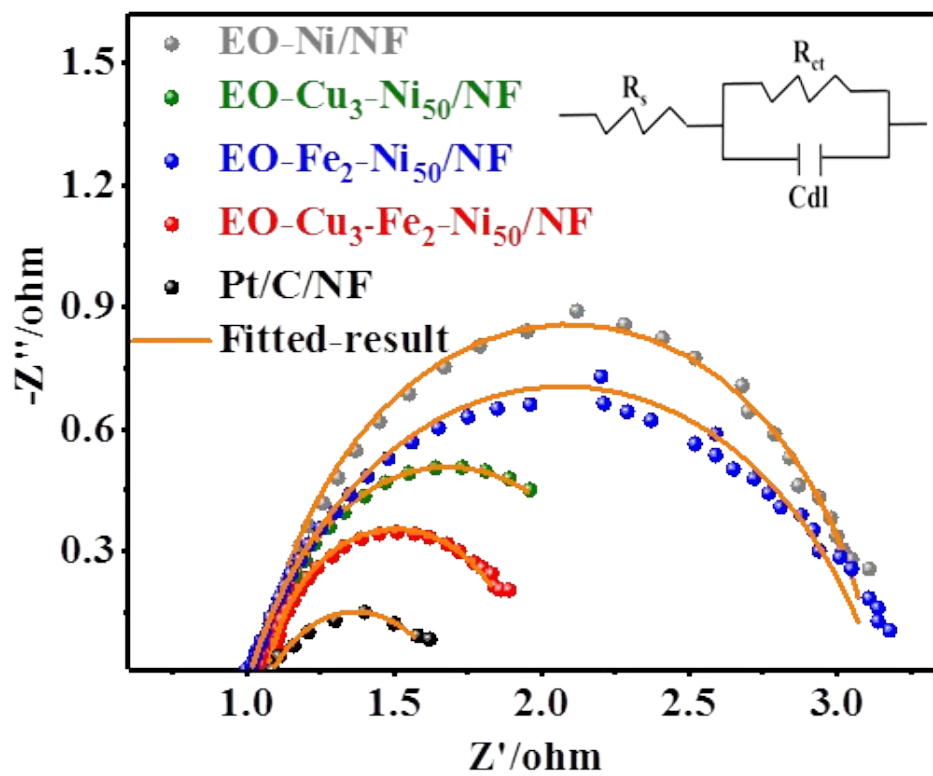


**Figure S11.** The equivalent circuits and the detail simulated results in EIS for HER.

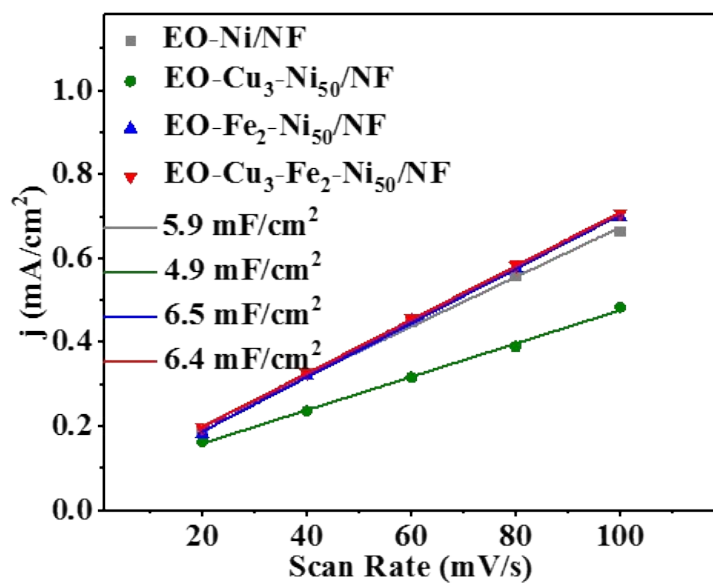


**Figure S12.** The electrochemical double-layer capacitances ( $C_{dl}$ ) of EO-Ni/NF, EO-Cu<sub>3</sub>-Ni<sub>50</sub>/NF, EO-Fe<sub>2</sub>-Ni<sub>50</sub>/NF and EO-Cu<sub>3</sub>-Fe<sub>2</sub>-Ni<sub>50</sub>/NF for HER.

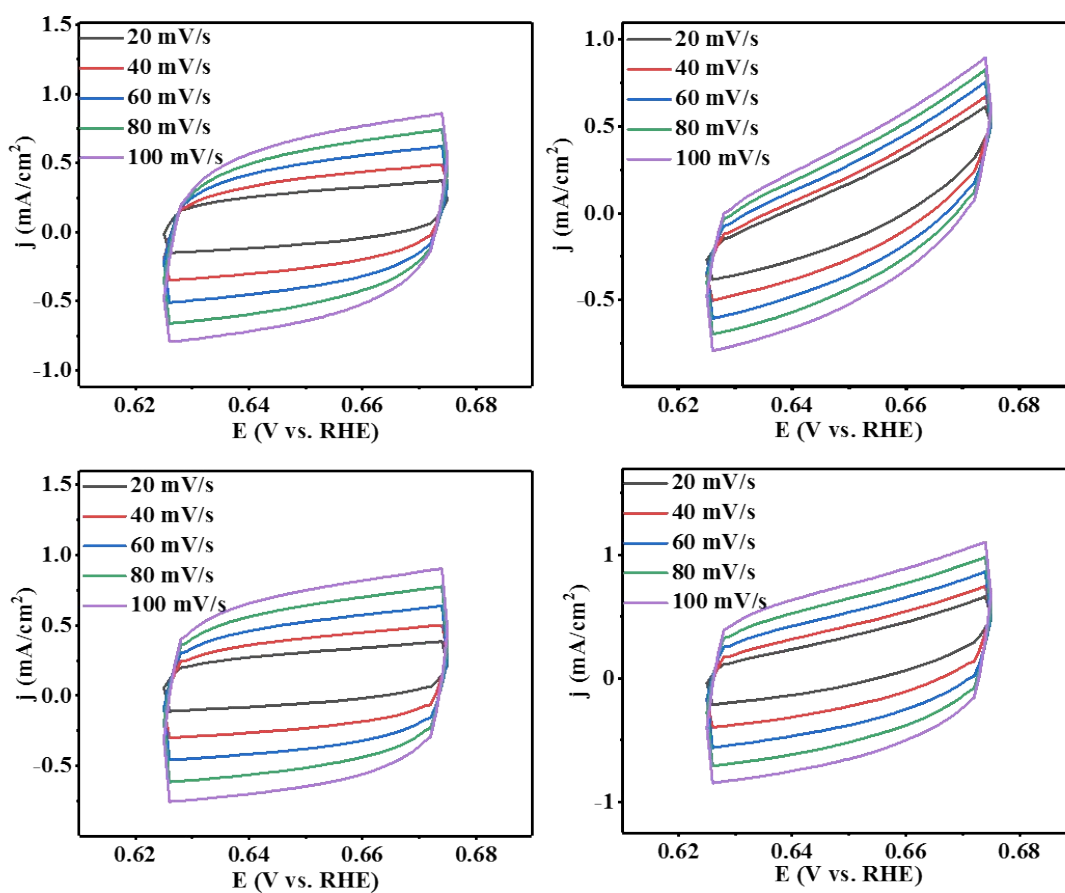


**Figure S13.** The CVs of (a) EO-Ni/NF, (b) EO-Cu<sub>3</sub>-Ni<sub>50</sub>/NF, (c) EO-Fe<sub>2</sub>-Ni<sub>50</sub>/NF and (d) EO-Cu<sub>3</sub>-Fe<sub>2</sub>-Ni<sub>50</sub>/NF at different scan rates in the non-Faraday region (0.625 ~0.675 V).

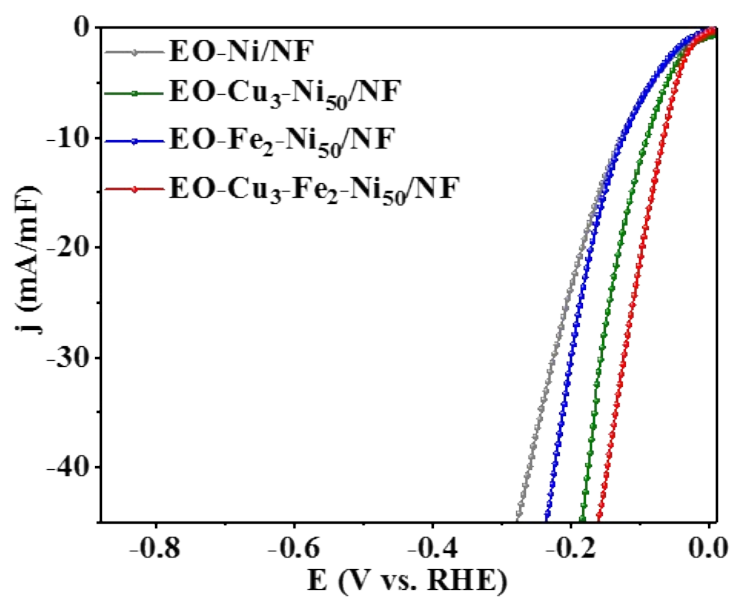


**Figure S14.** The normalized LSV curves of EO-Ni/NF, EO-Cu<sub>3</sub>-Ni<sub>50</sub>/NF, EO-Fe<sub>2</sub>-Ni<sub>50</sub>/NF and EO-Cu<sub>3</sub>-Fe<sub>2</sub>-Ni<sub>50</sub>/NF for HER by their respective  $C_{dl}$  values.



## Reference

[1]. Li, Y.; Tan, X.; Hocking, R. K.; Bo, X.; Ren, H.; Johannessen, B.; Smith, S. C.; Zhao, C., Implanting Ni-O-VO<sub>x</sub> sites into Cu-doped Ni for low-overpotential alkaline hydrogen evolution. *Nat. Commun.* **2020**, *11* (1), 2720.